Proceedings of the 10th IEEE International Conference on
Nano/Micro Engineered and Molecular Systems (IEEE-NEMS 2015)
Xi'an, China, April 7-11, 2015

Line Defect Detection on 2D materials with Micro Four-Point Probe Measurement

Xu Gong
Department of Electrical and Electronic Engineering,
South University of Science and Technology of China,
Shenzhen, China

Fei Wang [1,2]
[1] Department of Electrical and Electronic Engineering,
South University of Science and Technology of China,
Shenzhen, China (wangf@sustc.edu.cn)
[2] Shenzhen Key Laboratory of 3rd Generation Semiconductor Devices, Shenzhen, China

***Abstract*—This paper presents a measurement scheme which can be used to detect the line defects in two dimensional (2D) materials such as graphene. With micro four point probe measurement, the sheet resistances of the material can be mapped in two directions. Therefore, the line defects with insulation boundaries can be illustrated by calculating the resistance ratio R_A/R_B. We have demonstrated the simulations on 2D material with single defect and double defects with different positions and angles. The size effect of the defects has also been studied. The presented method is also promising for material characterization and defect estimation on film materials.**

Keywords—micro four point probe; 2D material; sheet resistance; boudary defect.

I. INTRODUCTION

There is an increasing research interest in the scalable production of high quality graphene material and devices. So far, the large scale graphene films are typically polycrystalline, where the electronic and magnetic properties are often affected by the grain boundaries (GB) [1-4]. It is generally difficult to detect the GB with an optical microscopy, and therefore, advanced transmission electron microscopy (TEM) is required.

Recently, micro four point probe measurement has been proven as an effective method for the characterization of sheet materials and fragile 2D materials such as silicon grass and graphene [5-6]. Since the measurement is sensitive to the local inhomogeneities [7-8], it may be useful to statistically detect the boundaries [9]. As shown in Figure 1, with two different probe configurations A and B, R_A and R_B can be measured on a film material. For a uniform film, the resistance ratio R_A/R_B is a constant when the probes scan across the sample. However, this ratio could be changed if there are line defects such as GB, which introduce insulation boundaries. In this paper, a detailed relationship between the line defects and the sheet resistance measurement is studied by finite element modeling.

II. SIMULATION

Similar to the sensitivity and accuracy studies on the sheet resistance measurement [10-11], the line defect measurement is also calculated by COMSOL modeling. Four-point probe

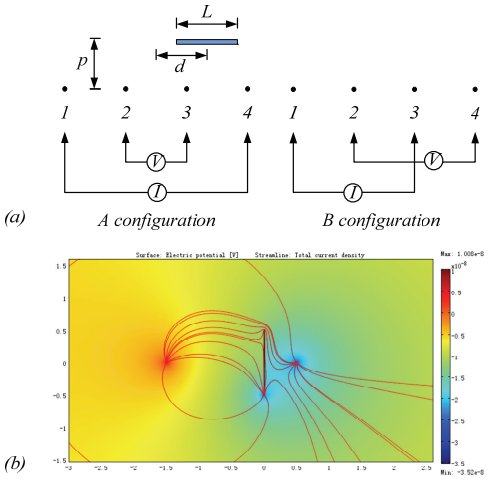

Figure 1: (a) Four point probe measurement on a sample with a line defect. L is the length of the defect; d is the distance between the center of the defect and the probe line; *p* is the probe pitch: (left) *A* configuration; (right) *B* configuration. (b) current distribution when there is a line defect on the sample.

with a probe pitch of p is firstly defined, then, an extremely high length-width ratio insulating area as line defect is set on an infinite large homogeneous film. The length of the line defect L is tuned from 0.5 p to 2 p with a step of 0.5 p during the simulation while the position of the defect can also be regulated. As shown in Figure 1(a), with different configurations of R_A and R_B measurements [10], a dimensionless ratio of R_A/R_B is defined. The current is applied from pin 1 to pin 4 in configuration A, and the potentials of pin 2 and 3 are extracted to calculate the voltage drop. In configuration B, the current is applied from pin 1 to pin 3, and the two remaining probes measure the voltage drop. The corresponding values of the ratio of voltage and current turn out to be R_A and R_B, respectively in each configuration. The resistance ratio R_A/R_B is only dependent on the length and the position of defect. Figure 1(b) shows the current distribution when there is a line defect in the 2D material.

Figures 2-3 have shown six typical cases of the line defects. The defect line can be aligned either parallel to the four-point probe or perpendicular to the probe line. For all the six typical cases, the R_A/R_B ratio stabilizes to a constant value of 1.26

978-1-4673-6695-3/15/$31.00 ©2015 IEEE

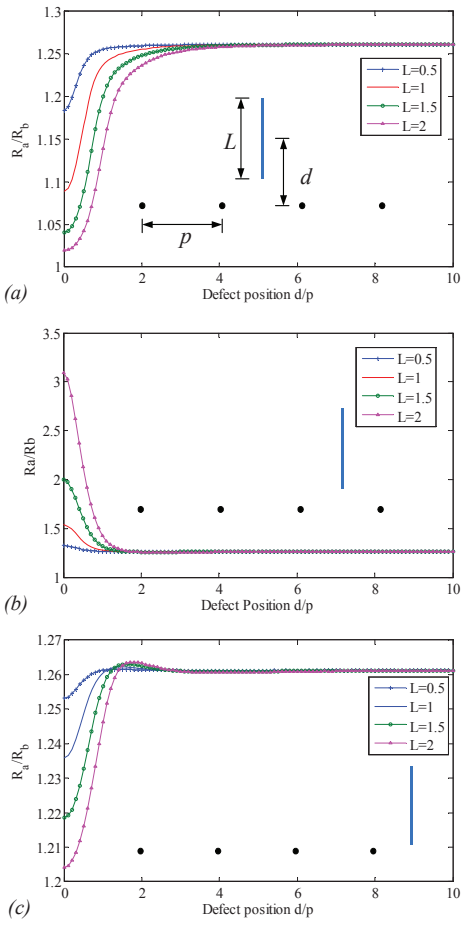

Figure 2: Single perpendicular line defect moving upwards from (a) the center of the probes; (b) x=p; (c) x=2p.

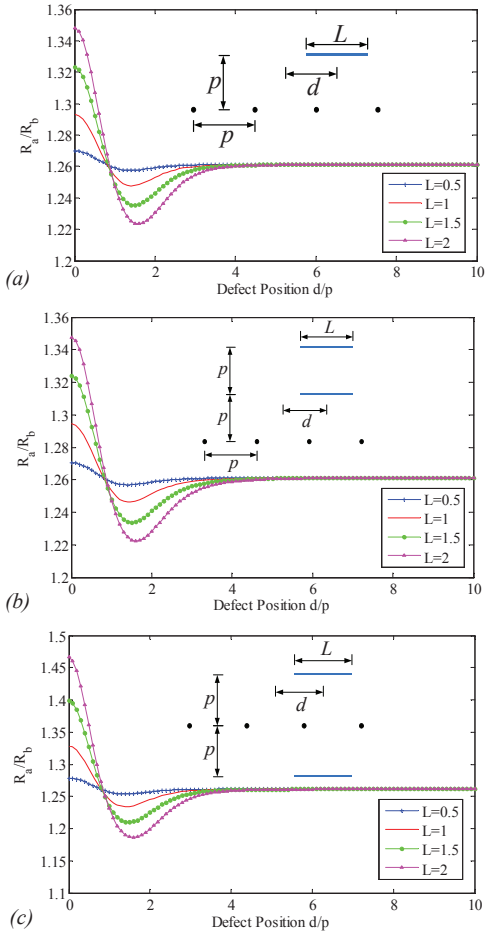

Figure 3. Line defect moving from d=0 to d=10p (with x=0 for the center of the probe) for (a) single defect; (b) two defects in the same side; (c) two defects in both sides.

when the four-point probe is far away from the line defect (~ 4p), which agrees well with the typical four point probe measurements on an infinite film. On the other hand, the R_A/R_B ratio could be very sensitive to the length and the position of the defect when the four-point probe is close to it. For instance, when the line defect locates at the center of the outer two probes, the R_A/R_B ratio goes up to 3.0 for a defect length of 2 p. The sensitivity of the R_A/R_B ratio on the defect size and position provides a possible method to detect the defects on the 2D material.

III. MAPPING

For line defect detection on 2D materials, a sheet resistance mapping procedure is necessary. During the mapping simulation, we first define the line defects on the 2D material, then we scan the sample with micro four point probes in two directions and record the sheet resistance measured for R_A and R_B. The resistance ratio R_A/R_B or R_B/R_A (to avoid singularity) is then calculated. From the mapping plots of the resistance ratio, we can detect the position and the size of the line defects on the sample.

Figure 4 shows a line defect detected by a 2D mapping of R_B/R_A measurement where the probe line is perpendicular to the defect line. From the 3D surface plot shown in Fig.4(a),

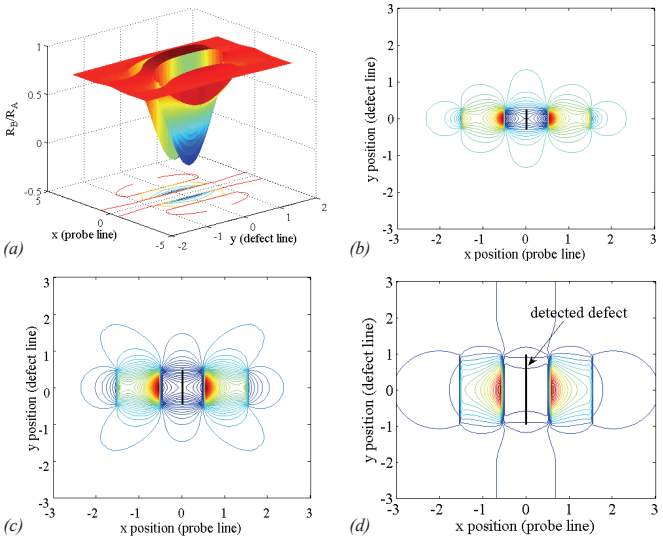

Figure 4. (a) The resistance ratio of R_B/R_A varies when the micro four point probes scan across the 2D sample with the probe line perpendicular to the defect line; (b-d) contour map of R_B/R_A where the line defect with a length of 0.5p, 1p, 2p is clearly seen.

we can clear see that R_B/R_A is highly dependent on the probe position. The R_B/R_A ratio decreases rapidly when the probes

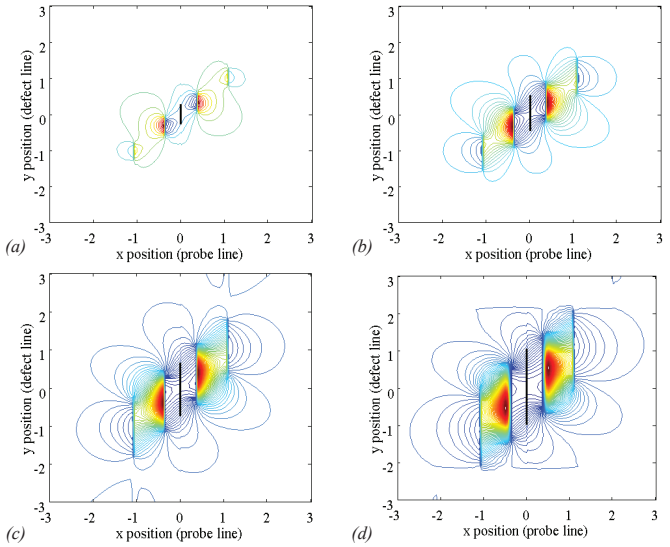

Figure 5. Contour map of R_B/R_A when the micro four point probes scan across the 2D sample with the probe line rotate by 45° from the defect with length of (a) 0.5p; (b)1p; (c)1.5p; and (d)2p.

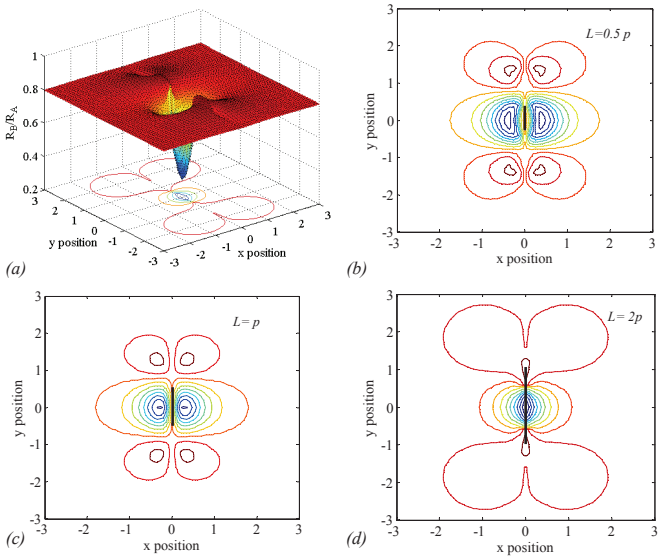

Figure 6. (a) Surface contour map of R_B/R_A when the micro four point probes scan across the 2D sample with the probe line parallel to the defect with a length of 2p. (b-d) Detailed contour map of R_B/R_A where the defect line can be detected while the length is not obvious.

go close to the defect. This is the boundary effect of the sheet resistance measurement as discussed in [11]. And since the A configuration and the B configuration use two different set of the probe pins setup, the boundary effect on R_A and R_B are different. In the contour maps of Fig.4(b-d), the position and the size of the line defect can be measured. More relative positions between the defects and the probe line have also been studied in the simulation. Figure 5 shows the contour map of the resistance ratio R_B/R_A when the probe line is 45° to the defect line. From the contour maps, the line defects with length of 0.5p, 1p, 1.5p and 2p can be detected. In Figure 6, micro four point probe scans across the sample with the probe line parallel to the defect line. From the contour map in

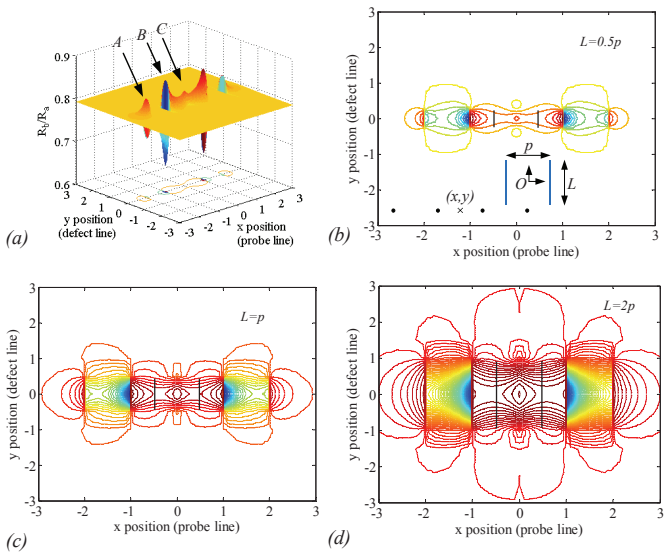

Figure 7. (a) Surface contour map of R_B/R_A when the micro four point probes scan across the 2D sample with the probe line perpendicular to two parallel defects which are 0.5p long and separated by p. (b-d) Detailed contour map of R_B/R_A for the two defect with lengths of 0.5p, 1p, and 2p.

Fig.6(b-d), the defect line can be detected while the length of the defect line is difficult to estimate.

Very often in practical 2D materials, there are more than single boundary defects. Therefore, double defects are also investigated in this work. Figure 7 shows the 2D mapping results of micro four point probe measurement on samples with double parallel line defects with a distance of *p*. The length of the defect lines are defined as 0.5p, 1p, and 2p, respectively. From the surface contour plot in Fig.7(a), the boundary effect on the variation of the resistance ratio R_B/R_A is compounded of two single line defects. The peak A occurs when the outer probe approaches the first defect where the resistances of R_A and R_B are sensitive to the boundary condition. When the probes scans further in x direction where the inner probe approaches the first defect, the peak B occurs which is typically more significant than the peak A. This is mainly due to the fact that the resistance sensitivity of R_A and R_B is more significant for the inner two probes which has been investigated in our previous work [10]. The peak C occurs when the two inner probes approach the two line defects. Since the probes are at the same side of the two defects, the sensitivities counteract with each other and therefore it is a minor peak. The contour maps in Fig.7(b-d) show the detailed variation of the resistance ratio where the line defects can be detected. Similar to the cases of single defects, the lengths of the defect can also be measured since the probes scan perpendicular to the defect lines.

IV. Conclusion

We have studied the effect of the boundary defects on the sheet resistance measurement. From the simulations of micro four-point probe measurement on 2D materials with single and double line defects, we have calculated the sensitivity of the resistance ratio R_A/R_B (or R_B/R_A) on the size and the location of defects. The variation of the resistance ratio can provide the

information of the defect condition, which is helpful to illustrate the defects and to characterize the 2D material such as graphene and other semiconductor film materials.

ACKNOWLEDGMENT

The authors would like to thank the financial support from Research Project JCYJ20140417105742703.

REFERENCES

[1] Q. Yu, L. A. Jauregui, W. Wu, R. Colby, J. Tian, Z. Su, H. Cao, Z. Liu, D. Pandey, D. Wei, T. F. Chung, P. Peng, N. P. Guisinger, E. A. Stach, J. Bao, S.-S. Pei, and Y. P. Chen, "Control and characterization of individual grains and grain boundaries in graphene grown by chemical vapour deposition," *Nat Mater*, vol. 10, no. 6, pp. 443–449, 2011.

[2] P. Y. Huang, C. S. Ruiz-Vargas, A. M. van der Zande, W. S. Whitney, M. P. Levendorf, J. W. Kevek, S. Garg, J. S. Alden, C. J. Hustedt, Y. Zhu, J. Park, P. L. McEuen, and D. A. Muller, "Grains and grain boundaries in single-layer graphene atomic patchwork quilts," *Nature*, vol. 469, no. 7330, pp. 389–392, 2011.

[3] D. W. Kim, Y. H. Kim, H. S. Jeong, and H.-T. Jung, "Direct visualization of large-area graphene domains and boundaries by optical birefringency," *Nature Nanotechnology*, vol. 7, no. 1, pp. 29–34, 2012.

[4] A. W. Tsen, L. Brown, M. P. Levendorf, F. Ghahari, P. Y. Huang, R. W. Havener, C. S. Ruiz-Vargas, D. A. Muller, P. Kim, and J. Park, "Tailoring Electrical Transport Across Grain Boundaries in Polycrystalline Graphene," *Science*, vol. 336, no. 6085, pp. 1143–1146, Jun. 2012.

[5] D. H. Petersen, F. Wang, M. B. Olesen, R. Wierzbicki, M. S. Schmidt, P. F. Nielsen, P. Boggild, O. Hansen, and K. Molhave, "Micro-cantilevers for non-destructive characterization of nanograss uniformity," in *Solid-State Sensors, Actuators and Microsystems Conference (TRANSDUCERS), 2011 16th International*, 2011, pp. 1060 –1063.

[6] F. Wang, D. H. Petersen, H. V. Jensen, C. Hansen, D. Mortensen, L. Friis, and O. Hansen, "Three-way flexible cantilever probes for static contact," *Journal of Micromechanics and Microengineering*, vol. 21, p. 085003, Aug. 2011.

[7] D. W. Koon, F. Wang, D. H. Petersen, and O. Hansen, "Sensitivity of resistive and Hall measurements to local inhomogeneities," *Journal of Applied Physics*, vol. 114, no. 16, p. 163710, Oct. 2013.

[8] D. W. Koon, F. Wang, D. H. Petersen, and O. Hansen, "Sensitivity of resistive and Hall measurements to local inhomogeneities: Finite-field, intensity, and area corrections," *Journal of Applied Physics*, vol. 116, no. 13, p. 133706, Oct. 2014.

[9] J. D. Buron, D. H. Petersen, P. Bøggild, D. G. Cooke, M. Hilke, J. Sun, E. Whiteway, P. F. Nielsen, O. Hansen, A. Yurgens, and P. U. Jepsen, "Graphene Conductance Uniformity Mapping," *Nano Lett.*, vol. 12, no. 10, pp. 5074–5081, 2012.

[10] F. Wang, D. H. Petersen, T. M. Hansen, T. R. Henriksen, P. Boggild, and O. Hansen, "Sensitivity study of micro four-point probe measurements on small samples," *J. Vac. Sci. Technol. B*, vol. 28, no. 1, p. C1C34, 2010.

[11] S. Thorsteinsson, F. Wang, D. H. Petersen, T. M. Hansen, D. Kjær, R. Lin, J.-Y. Kim, P. F. Nielsen, and O. Hansen, "Accurate microfour-point probe sheet resistance measurements on small samples," *Rev. Sci. Instrum.*, vol. 80, no. 5, p. 053902, 2009.